

# PV Power Output Variability: Correlation Coefficients

---

Thomas E. Hoff and Richard Perez  
Clean Power Research  
[www.cleanpower.com](http://www.cleanpower.com)  
Draft, November 11, 2010

## Abstract

Utility planners and operators are responsible for guiding where PV systems are located and are accountable for system reliability. They are concerned about how short-term PV system output changes may affect utility system stability. That is, they are concerned about PV power output variability.

This paper introduces a novel approach to estimate the maximum short-term output variability that a fleet of PV systems places on any considered power grid. A key input to this approach is the correlation, or absence thereof, existing between individual installations in the fleet at the considered variability time scale.

Short-term PV power output variability is driven by changes in the clearness index. Thus, the paper focuses on analyzing the correlation coefficient of the change in the clearness index between two locations as a function of distance, time interval, and other parameters. The paper presents a method to estimate correlation coefficients that uses location-specific input parameters. The method appears to be capable of describing site-pair correlation across time intervals from seconds to hours.

The method is derived empirically and validated using 12 years of hourly satellite-derived data from SolarAnywhere® in three geographic regions in the United States (Southwest, Southern Great Plains, and Hawaii). Results at time intervals less than one hour are corroborated using findings from recent investigations that were based on 10-second to one-minute data sets.

The strength and structure of the method is summarized by three fundamental findings that both confirm and extend conclusions from previous studies:

1. Correlation coefficients decrease predictably with increasing distance.
2. Correlation coefficients decrease at a similar rate when evaluated versus distance divided by the considered variability time interval.
3. The accuracy of results is improved by including an implied cloud speed term.

The present approach has potential financial benefits to systems that are concerned about PV power output variability, ranging from distribution feeders to balancing regions.

## Introduction

PV capacity is increasing on utility systems. As a result, utility planners and operators are growing more concerned about potential impacts of power supply variability caused by transient clouds. Utilities and control system operators need to adapt their planning, scheduling, and operating strategies to accommodate this variability while at the same time maintaining existing standards of reliability.

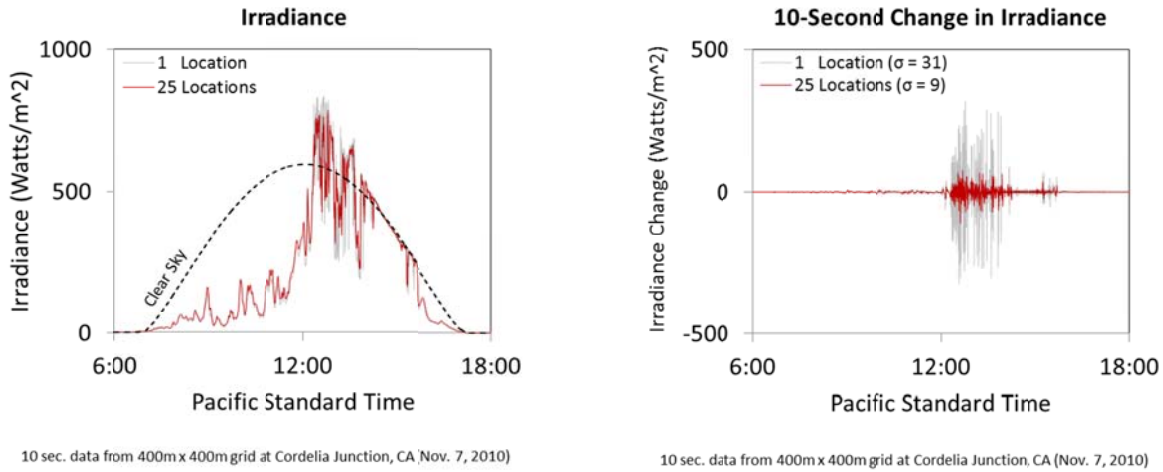
It is impossible to effectively manage these systems, however, without a clear understanding of PV output variability or the methods to quantify it. Whether forecasting loads and scheduling capacity several hours ahead or planning for reserve resources years into the future, the industry needs to be able to quantify expected output variability for fleets of up to hundreds of thousands of PV systems spread across large geographical territories. Underestimating reserve requirements may result in a failure to meet reliability standards and an unstable power system. Overestimating reserve requirements may result in an unnecessary expenditure of capital and higher operating costs.

The present objective is to develop analytical methods and tools to quantify PV fleet output variability. Variability in time intervals ranging from a few seconds to a few minutes is of primary interest since control area reserves are dispatched over these time intervals. For example, regulation reserves might be dispatched at an ISO every five seconds through a broadcast signal. Knowledge about PV fleet variability in five-second intervals could be used to determine the resources necessary to provide frequency regulation service in response to power fluctuations.

Variability of a PV fleet is thus a measure of the magnitude of changes in its aggregate power output corresponding to the defined time interval and taken over a representative study period. Note that it is the *change* in output, rather than the output itself, that is desired. Also note that, for each time interval the change in output may vary in both magnitude and sign (positive and negative). A statistical metric is therefore employed in order to quantify variability: the *standard deviation of the change in fleet power output*.

It is helpful to graphically illustrate what is meant by output variability. The left side of Figure 1 presents 10-second irradiance data (PV power output is almost directly proportional to irradiance) and the right side of the figure presents the change in irradiance using a 10-second time interval for a network of 25 weather monitoring stations in a 400-meter by 400-meter grid located at Cordelia Junction, CA on November 7, 2010 (Hoff and Norris, 2010). The light gray lines correspond to irradiance and variability for a single location and the dark red lines correspond to average irradiance distributed across 25 locations. Results suggest that spreading capacity across 25 locations rather than concentrating it at a single location reduces variability by more than 70 percent in this particular instance.

Figure 1. Twenty-five location network reduces 10-second variability by more than 70 percent in a 400 meter x 400 meter grid at Cordelia Junction, CA on November 7, 2010.



A “fleet computation” approach can be taken to calculate output variability for a fleet of PV systems as follows: identify the PV systems that constitute the fleet to be studied; select the time interval and time period of concern (e.g., one-minute changes evaluated over a one-year period); obtain time-synchronized solar irradiance data for each location where a PV system is to be sited; simulate output for each PV system using standard modeling tools; sum the output from each individual system to obtain the combined fleet output; calculate the change in fleet output for each time interval; and finally calculate the resulting statistical output variability from the stream of values.

This “fleet computation” approach, while technically valid, is difficult to implement in practice for several reasons. First, insolation data is not available in sufficient resolution (either time resolution or geographical resolution). For example, SolarAnywhere (2010), which provides operational real-time insolation data for the continental U.S. and Hawaii, is currently based on a 10 km x 10 km grid and a one-hour time interval. It has a practical real-time limit of one-half hour and a few km based on current satellite technology. Fleet computation could not be performed for, say, systems spaced 0.5 km apart with a four-minute time interval. Second, PV variability determined using the fleet computation approach is only applicable to studies having a matching time interval of interest and a fixed fleet selection. The study would have to be re-commissioned whenever additional PV systems came on-line. Finally, calculations are highly computation intensive, and thus are not suitable for real-time operations.

A more viable approach is to streamline the calculations through the use of a general-purpose PV output variability methodology. The method needs to quantify short-term fleet power output variability using the observations that sky clearness and sun position drive the changes in the short-term output for individual PV systems and that physical parameters (i.e., dimensions, plant spacing, number of plants, etc.) determine overall fleet variability.

Hoff and Perez (2010) developed a simplified model as a first step towards a general method to quantify the output variability resulting from an ensemble of equally-spaced, identical PV systems. They defined

output variability to be the standard deviation of the change in output over some time interval (such as one minute), using data taken from some time period (such as one year).

The simplified model covered the special case when the change in output between locations is uncorrelated (i.e., cloud impacts at one site are too distant to have predictable effects at another for the considered time scale), fleet capacity is equally distributed, and the variance at each location is the same. Under these conditions, Hoff and Perez showed that fleet output variability equals the output variability at any one location divided by the square root of the number of locations:<sup>1</sup>

$$\sigma_{\Delta t}^{Fleet} = \frac{\sigma_{\Delta t}^1}{\sqrt{N}} \quad (1)$$

where  $\sigma_{\Delta t}^{Fleet}$  is the standard deviation of the change in output of the fleet using a time interval of  $\Delta t$ ,  $\sigma_{\Delta t}^1$  is the standard deviation of the change in output of the fleet concentrated at a single location, and  $N$  is the number of uncorrelated locations.

Mills and Wiser (2010) have derived a similar result that relates variability to the square root of the number of systems when the locations are uncorrelated.

## Maximum Output Variability

Equation ( 1 ) has important implications for utility planners. It allows them to determine reserve capacity requirements to mitigate worst case fleet variability. For example, suppose that the variability of a single system was 10 kW per minute and there were 100 uncorrelated identical systems in the fleet. Total fleet variability equals 0.1 MW ( $\frac{100 \cdot 10 \text{ kW}}{\sqrt{100}}$ ) per minute. The planner could then apply the desired confidence level (e.g., they may choose 3 standard deviations) to determine the required reserve capacity (e.g., 3 x 0.1 MW = 0.3 MW).

This calculation is applicable when two fundamental conditions are satisfied: (1) the output variability at a single location can be quantified and (2) the change in output variability between locations is uncorrelated.

Consider the first condition. One approach to determining single location variability ( $\sigma_{\Delta t}^1$ ) is to analyze historical solar resource data for the location of interest. The data would need to have been collected at a rate that accommodates the time interval of interest (perhaps down to a few seconds) over a substantial and representative period of time (perhaps over several years). Such high-speed, high-resolution data is not generally available.<sup>2</sup>

An alternative approach is to construct a data set that simulates worst case variability conditions. The theoretically worst case variability of a single PV plant would be that it cycles alternately between 0 and 100 percent of its rated output every time interval. For example, suppose that the PV plant is rated at 1

---

<sup>1</sup> See Equation (8) in Hoff and Perez (2010).

<sup>2</sup> One of the few examples of this sort of data is provided by Kuszamaul, et. al. (2010).

MW and the time interval of interest is 1 minute. As illustrated in Table 1, maximum variability occurs when the PV plant is at full power at 12:00, zero power at 12:01, full power at 12:02, etc. As illustrated in the right side of the table, the corresponding change in power fluctuates between -1 and 1 MW. The standard deviation<sup>3</sup> of the change in power output equals 1 MW per minute. That is, a 1 MW PV plant that is exhibiting maximum variability over a 1 minute time interval has a 1 MW per minute standard deviation. This would imply that 1 MW of reserve capacity is required to compensate for the output variability for a single plant.

Table 1. Maximum change in power output at one location.

Time	Power (MW)	Change (MW/min)
12:00	1	-1
12:01	0	+1
12:02	1	-1
12:03	0	+1
12:04	1	

Suppose that the PV “fleet” capacity was split between two locations and each were to exhibit maximum output variability. Two possible scenarios exist. The first scenario, illustrated in Table 2, assumes that both plants turn on and off simultaneously. As was the case where all capacity is concentrated at a single location, the change in output fluctuates between -1 and 1 MW and the standard deviation for this scenario is 1 MW per minute.

The second scenario, illustrated in Table 3, assumes that the plants cycle on and off alternately with a time shift of 1 minute. In this case, the change in output from the first location cancels the change in output at the second location. The result of this scenario is a standard deviation of 0 MW per minute.

It is incorrect to conclude, however, that the upper bound of output variability for 1 MW of PV is 1 MW per minute because this is the larger value of the two scenarios (the first equals 1 MW per minute and the second equals 0 MW per minute). This is because each of the two scenarios violates the assumed condition that the locations are uncorrelated. Specifically, the change in output between the two locations has perfect positive correlation in the first scenario (i.e., correlation coefficient equals 1) and perfect negative correlation in the second scenario (i.e., correlation coefficient equals -1).

---

<sup>3</sup> The standard deviation of a random variable **X** equals the square root of the expected value of X squared minus the square of the expected value of X.  $\sigma = \sqrt{E[X^2] - E[X]^2}$ .

Table 2. Maximum change in power output at two locations (scenario 1).

Time	Power (MW)			Change (MW/min)
	Plant 1	Plant 2	Fleet (1+2)	
12:00	0.5	0.5	1	- 1
12:01	0	0	0	+1
12:02	0.5	0.5	1	-1
12:03	0	0	0	+1
12:04	0.5	0.5	1	

Table 3. Maximum change in power output at two locations (scenario 2).

Time	Power (MW)			Change (MW/min)
	Plant 1	Plant 2	Fleet 1+2	
12:00	0.5	0	0.5	0
12:01	0	0.5	0.5	0
12:02	0.5	0	0.5	0
12:03	0	0.5	0.5	0
12:04	0.5	0	0.5	

### Feasible Maximum Output Variability

These scenarios demonstrate that it is impossible for two systems to exhibit the behavior of worst case variance individually (by cycling on and off at each interval) without having either perfect positive or perfect negative correlation. Indeed, for each system to exhibit its maximum variance, its output changes must be exactly in tempo with the time interval, loosely analogous to each member of an orchestra following in time to its conductor, in which case the systems would by definition have perfect correlation (whether positive or negative). By this reasoning, the maximum output variability scenario described above (1 MW of variability for each 1 MW of fleet capacity) is impossible. When the systems have less than perfect correlation, as must be the case for any real-world fleet, the variability of the combined fleet must be less than the total fleet capacity.

To correct the worst case scenario, retain the assumption that each power change is either a transition from zero output to full output or from full output to zero output. This assumption in itself is highly conservative since the impacts of cloud transients on PV systems will almost never produce changes with magnitudes as high as 100 percent of rated output and will generally produce changes much less than 100 percent. As for timing, rather than being synchronized, each system is assumed to cycle on and off in a random fashion, representing fleets of PV systems with outputs that are uncorrelated.

Random timing of power output changes is illustrated for a single location in Table 4 for a 1 MW PV system. Suppose that it is 12:00 and the time interval is 1 minute. There is a 50 percent chance that the

plant is on and a 50 percent chance that the plant is off at 12:00. If the plant is on at 12:00, then there is a 50 percent chance it will turn off and a 50 percent chance it will remain on at 12:01. If the plant is off at 12:00, then there is a 50 percent chance it will stay off and a 50 percent chance it will turn on at 12:01. The right column in Table 4 presents the probability distribution of the change in power. At each time interval, there is a 25 percent chance of a 1 MW per minute decrease in power, a 50 percent chance of no change in output, and a 25 percent chance of a 1 MW per minute increase in power.

Note that while this is the maximum possible change, it is extremely unlikely that such a distribution would actually exist. First, weather conditions would have to be exceptionally erratic. Second, clouds would need to be so dark that there would be no output when covering a PV system. Third, the entire system would have to turn on and off, rather than a subset of the arrays. Fourth, each PV system would need to operate as a “point source” of output; Kuszamaul et. al. (2010) and Mills et. al. (2009) have demonstrated that, in fact, a smoothing effect occurs as system size increases.<sup>4</sup>

Table 4. Maximum change in power output assuming random output.

Time	Power (MW)		Change (MW/min)
12:00	<div style="text-align: center;">50%</div> <div style="text-align: center;">Plant On (1)</div>		25% chance of 1 50% chance of 0 25% chance of -1
12:01	<div style="display: flex; justify-content: space-around;"> <div style="text-align: center;">50%</div> <div style="text-align: center;">50%</div> </div> <div style="display: flex; justify-content: space-around;"> <div style="text-align: center;">Plant Off (0)</div> <div style="text-align: center;">Plant On (1)</div> </div>		
	<i>Scenario 1</i>		
	<i>Scenario 2</i>		

With these caveats, the above distribution is taken for the current purposes. This distribution has a standard deviation of  $\frac{1}{\sqrt{2}}$  times 1 MW.<sup>5</sup> If the entire fleet of PV systems were concentrated at a single point, and the fleet had a capacity of  $C^{Fleet}$ , then the maximum standard deviation of change in output equals:

$$\text{Maximum } \sigma_{\Delta t}^1 = \frac{C^{Fleet}}{\sqrt{2}} \quad (2)$$

The maximum output variability for a fleet of uncorrelated locations can be calculated using this numerical definition of the maximum output variability for a single system by substituting Equation ( 2 ) into Equation ( 1 ).The result is that that maximum output variability equals fleet capacity divided by the square root of 2 times the number of uncorrelated locations.

$$\text{Maximum } \sigma_{\Delta t}^{Fleet} = \frac{C^{Fleet}}{\sqrt{2N}} \quad (3)$$

<sup>4</sup> See Figure 13 in Kuszamaul et. al. (2010) and Figure 7 in Mills et. al. (2009).

<sup>5</sup>  $\sigma = \sqrt{[(0.25)(-1)^2 + (0.50)(0)^2 + (0.25)(1)^2] - [(0.25)(-1) + (0.50)(0) + (0.25)(1)]^2} = \frac{1}{\sqrt{2}}$

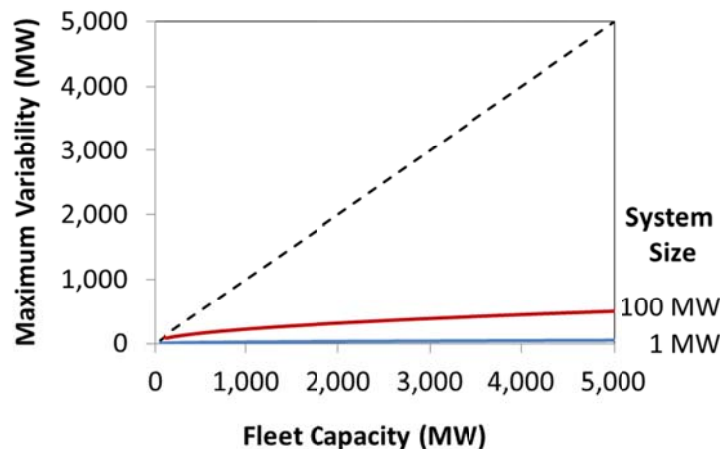
Equation ( 3 ) places an upper bound on the maximum output variability for any time interval as long as the change in output between locations is uncorrelated. Actual results are likely to be lower. This practical upper bound on single point output is substantiated by a wealth of empirical evidence (see Perez et al., 2010a).

### Example

Suppose that a utility system plans to incorporate 5,000 MW of PV. Figure 2 presents the maximum output variability calculated using Equation ( 3 ) for PV fleets with capacities ranging from 0 to 5,000 MW based on two fleet composition strategies. The blue line is the variability when the fleet is composed of uncorrelated 1 MW systems. The red line is the variability when the fleet is composed of uncorrelated 100 MW systems. As illustrated in the figure at the 5,000 MW level, if 100 MW systems are installed at 50 locations (N=50) with uncorrelated changes in output, maximum output variability is 500 MW per time interval, or 10 percent of fleet capacity. However, if 1 MW PV systems are installed at 5,000 locations (N=5,000) with uncorrelated changes in output, maximum output variability is 50 MW, or 1 percent of fleet capacity.<sup>6</sup>

This example illustrates the potential benefit of dividing the PV capacity into small systems, and spreading them apart geographically so that output changes are uncorrelated. More importantly, it also illustrates the unnecessary potential cost that could be incurred if system planners were to procure reserves without adequate tools for quantifying PV variability. The dotted line represents the reserve resources that would be procured when each MW of PV was fully “backed up” with a MW of fossil, battery, or other dispatchable resource. In the N=5,000 example, such a planning practice — at least for fleets made up of uncorrelated systems— would result in capital expenditures 99 times the required amounts.

Figure 2. Maximum variability for 1 MW and 100 MW system sizes with uncorrelated changes.



<sup>6</sup> Appendix A illustrates how to verify these results using an Excel spreadsheet.



## Correlation versus Distance

### Background: Critical Factors Affecting Correlation

The critical factors that affect output variability are the clearness of the sky, sun position, and PV fleet orientation (i.e., dimensions, plant spacing, number of plants, etc.). To improve accuracy, Hoff and Perez (2010) introduced a parameter called the Dispersion Factor. The Dispersion Factor is a parameter that incorporates the layout of a fleet of PV systems, the time scales of concern, and the motion of cloud interferences over the PV fleet. Hoff and Perez demonstrated that relative output variability resulting from the deployment of multiple plants decreased quasi-exponentially as a function of the generating resource's Dispersion Factor. Their results demonstrated that relative output variability (1) decreases as the distance between sites increases; (2) decreases more slowly as the time interval increases; and (3) decreases more slowly as the cloud transit speed increases.

Mills and Wiser (2010) analyzed measured one-minute insolation data over an extended period of time for 23 time-synchronized sites in the Southern Great Plains network of the Atmospheric Radiation Measurement (ARM) program. Their results demonstrated<sup>7</sup> that the correlation of the change in the global clear sky index (1) decreases as the distance between sites increases and (2) decreases more slowly as the time interval increases.

Perez et. al. (2010b) analyzed the correlation between the variability observed at two neighboring sites as a function of their distance and of the considered variability time scale. The authors used 20-second to one-minute data to construct virtual networks at 24 US locations from the ARM program (Stokes and Schwartz, 1994) and the SURFRAD Network and cloud speed derived from SolarAnywhere (2010) to calculate the station pair correlations for distances ranging from 100 meters to 100 km and from variability time scales ranging from 20 seconds to 15 minutes. Their results demonstrated that the correlation of the change in global clear sky index (1) decreases as the distance between sites increases and (2) decreases more slowly as the time interval increases.

The consistent conclusions<sup>8</sup> of these studies are that correlation: (1) decreases as the distance between sites increases and (2) decreases more slowly as the time interval increases. Hoff and Perez (2010) add that the correlation decreases more slowly as the speed of the clouds increases.

### Objective

Utility planners clearly require a tool that can reliably quantify the maximum output variability of PV fleets using a manageable amount of data and analysis. Equation ( 3 ) would potentially meet this requirement if the change in output between locations were uncorrelated (i.e., correlation coefficient is zero). In real fleets, PV systems will generally have some degree of correlation, so any planning tool will have to incorporate correlation effects in calculating actual fleet variability.

This paper takes a step towards a general method by analyzing the correlation coefficient of the change in clearness index between two locations as a function of distance, time interval, and other parameters.

---

<sup>7</sup> See Figure 5 in Mills and Wiser (2010).

<sup>8</sup> The results apply to either changes in PV output directly or changes in the clear sky index

It uses hourly global horizontal insolation data from SolarAnywhere (2010) to calculate correlation coefficients for 70,000 scenarios across three separate geographic regions in the United States (Southwest, Southern Great Plains, and Hawaii). The correlation coefficients taken from these scenarios are then compared to a method that could prove useful when integrated into utility planning and operations tool. Recognizing that the method must also be validated for shorter time intervals (several seconds to several minutes), its results are compared to studies based on 10-second, 20-second, and 1-minute insolation data sets.

## Approach

Hoff and Perez (2010) defined PV fleet variability as the standard deviation of its power output changes using a selected sampling time interval (e.g., such as one minute or one hour) and analysis period (such as one year), as expressed relative to the fleet capacity. To simplify the work, they formulated it in terms of the change in insolation rather than the change in PV power.

As stated earlier, sky clearness and sun position drive the changes in short-term output for individual PV systems. Mills and Wiser (2010) and Perez, et. al (2010) subsequently isolated the random component of output change and examined changes attributable only to changes in global clear sky (or clearness) index. The global clearness index equals the measured global horizontal insolation divided by the clear sky insolation.

This paper continues in the direction of Mills and Wiser (2010) and Perez, et. al. (2010) and focuses on changes in the global clearness index.

## Change in Global Clearness Index

The global clearness index at a specific point in time is typically referred to as  $Kt^*$ . It equals the measured global horizontal insolation (GHI) divided by the clear-sky insolation. This paper refers to the change in the index between two points in time as  $\Delta Kt^*$ . Since the change occurs over some specified time interval,  $\Delta t$ , at some specific location  $n$ , the variable is fully qualified as  $\Delta Kt^*_{t,\Delta t}^n$ . This only represents one pair of points in time. A set of values is identified by convention by bolding the variable. Thus,  $\Delta Kt^*_{\Delta t}^n$  is the set of changes in the clearness indices at a specific location using a specific time interval over a specific time period.

$$\Delta Kt^*_{\Delta t}^n = \{(t_1, \Delta Kt^*_{t_1,\Delta t}^n), (t_2, \Delta Kt^*_{t_2,\Delta t}^n), \dots, (t_T, \Delta Kt^*_{t_T,\Delta t}^n)\} \quad (4)$$

Table 5 illustrates how to calculate the change in clearness index ( $\Delta Kt^*$ ) during conditions of rapidly changing insolation. For example,  $\Delta Kt^*$  between 12:00 and 12:01 equals the difference between  $Kt^*$  at 12:01 and  $Kt^*$  at 12:00 ( $0.5 - 1.0 = -0.5$ ).

Table 5. Example of how to calculate change in clearness index ( $\Delta Kt^*$ ) using  $\Delta t = 1$  minute.

Time	GHI	Clear-sky GHI	$Kt^*$	$\Delta Kt^*$
12:00	1.0	1.0	1.0	- 0.5
12:01	0.5	1.0	0.5	- 0.5
12:02	0.0	1.0	0.0	+0.5
12:03	0.5	1.0	0.5	+0.5
12:04	1.0	1.0	1.0	

Correlation and dependence in statistics are any of a broad class of statistical relationships between two or more random variables or observed data values (Wikipedia 2010). Let  $\Delta Kt^*_{\Delta t}^1$  and  $\Delta Kt^*_{\Delta t}^2$  represent two sets of observed data values for the change in the clearness index that have a mean of 0 and standard deviations,  $\sigma_1$  and  $\sigma_2$ .<sup>9</sup>

Pearson's product-moment correlation coefficient (typically referred to simply as the correlation coefficient) equals the expected value of  $\Delta Kt^*_{\Delta t}^1$  times  $\Delta Kt^*_{\Delta t}^2$  divided by the corresponding standard deviations.

$$\rho_{1,2} = \frac{E[\Delta Kt^*_{\Delta t}^1 \Delta Kt^*_{\Delta t}^2]}{\sigma_1 \sigma_2} \quad (5)$$

The analysis is performed as follows:

1. Select a geographic region for analysis
2. Select a location for the first part of the pair
3. Select a location for the second part of the pair
4. Select a time interval for the analysis
5. Select a clear sky irradiance level bin
6. Obtain detailed insolation data
7. Calculate the correlation coefficient<sup>10</sup>
8. Repeat the calculation for all sets of location pairs, time intervals, and clear sky irradiance bins.

<sup>9</sup> The expected value of  $\Delta Kt^*$  equals 0 as long as the starting and ending GHI values are the same. This condition is satisfied when the time period of the analysis is performed over one day because the starting and ending GHI both equal 0. It will also be approximately true when the analysis encompasses many data points (as would be the case, for example, of an analysis of one hour of data using a one-minute time interval).

<sup>10</sup> Appendix B illustrates how to calculate  $\Delta Kt^*$  correlation coefficients.


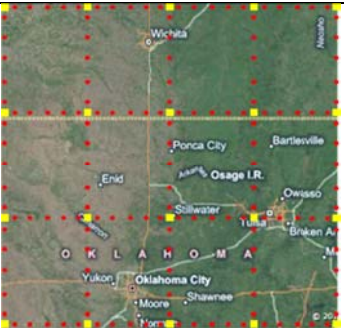

The focus of this paper is on trying to determine if patterns existing that help to better quantify correlation coefficients. As part of the objective, a method is tested that produces the desired output parameter of the correlation coefficient of the change in the clearness index between two separate locations. As discussed by Hoff and Perez (2010), the inputs into this method include the distance between the two locations, time interval, and location-specific parameters based on empirical weather data, in particular, cloud speed.

## Results

### Scenario Specification

As summarized in Table 6, three separate geographic regions in the United States were selected for analysis: Southwest, Southern Great Plains, and Hawaii. The first location (denoted by each of several yellow squares in the figures), was selected using a grid size of 2.0°, 1.0°, or 0.5° for the Southwest, Southern Great Plains, and Hawaii, correspondingly. The second location (denoted by a red circle in the figures) was selected between 0.1° and 2.9° (about 10 to 300 km) from the first location (other map coordinates were available but the illustrated points provided sufficient data and ease of analysis, so were ignored). Hourly insolation data was obtained for each of the two locations covering the period January 1, 1998 through September 30, 2010 from SolarAnywhere (2010). The analysis was then performed as described above for time intervals of 1, 2, 3, and 4 hours and for 10 separate clear sky irradiance bins. This analysis resulted in more than 70,000 correlation coefficients.

Table 6. Summary of input data.

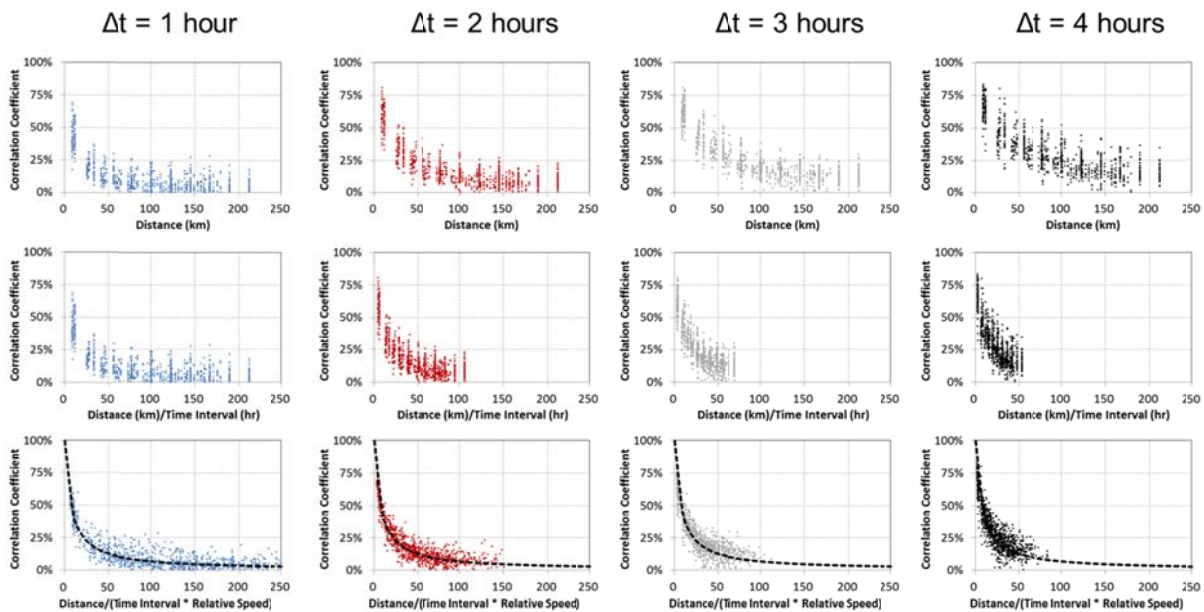
Region	Southwest	Southern Great Plains	Hawaii
			
<b>Location #1</b>	Latitude: 32° to 42° Longitude: -125° to -109° Grid Size: 2.0°	Latitude: 35° to 38° Longitude: -99° to -96° Grid Size: 1.0°	Latitude: 19° to 20° Longitude: -156° to -155° Grid Size: 0.5°
<b>Location #2</b>	0.1°, 0.3°, ..., 1.9° from #1	0.1°, 0.3°, ..., 2.9° from #1	0.1°, 0.2°, ..., 1.0° from #1
<b>Time Intervals</b>	1, 2, 3, and 4 hours	1, 2, 3, and 4 hours	1, 2, 3, and 4 hours
<b>Clear Sky Irradiance</b>	10 irradiance bins in intervals of 0.1 kW/m <sup>2</sup>	10 irradiance bins in increments of 0.1 kW/m <sup>2</sup>	10 irradiance bins in increments of 0.1 kW/m <sup>2</sup>

## Correlation Coefficients

Figure 3 presents the correlation coefficients for the Southwest.<sup>11</sup> The columns summarize the results for each time interval and the rows present the measured correlation coefficients versus several alternative candidate sets of variables. The first column summarizes results for a time interval of 1 hour. The second, third, and fourth columns plot the same results using time intervals of 2, 3, and 4 hours. Results in the top row present correlation coefficients versus the distance between the two locations. Results in the middle row present correlation coefficients versus distance divided by time interval. Results in the bottom row present correlation coefficients versus distance divided by time interval multiplied by relative speed;<sup>12</sup> this term is related to the Dispersion Factor introduced by Hoff and Perez (2010). The dashed line in the bottom figures represents the results of a generalized method, proposed in this paper for use in future tools, that will be validated in the present analysis. Results are calculated using parameters obtained from SolarAnywhere.

Figure 4 and Figure 5 present comparative results for the Great Plains and Hawaii. The patterns presented in the figures are similar across all time intervals in the three geographic locations. Figure 6 compresses the results for each location and presents results where all time intervals are combined into the same figure.

Figure 3. Correlation coefficients presented by time interval for Southwest.

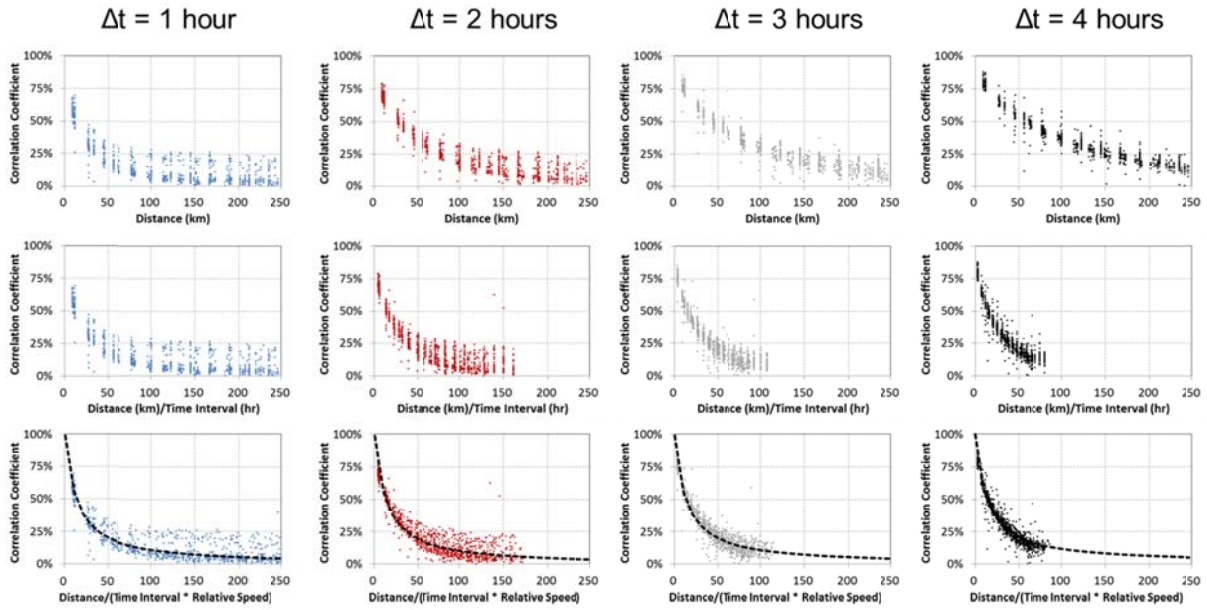


Note: Distance / (Time Interval \* Relative Speed) is related to Dispersion Factor

<sup>11</sup> The data in all of the figures represent randomly selected samples of points in order to make the results more readable.

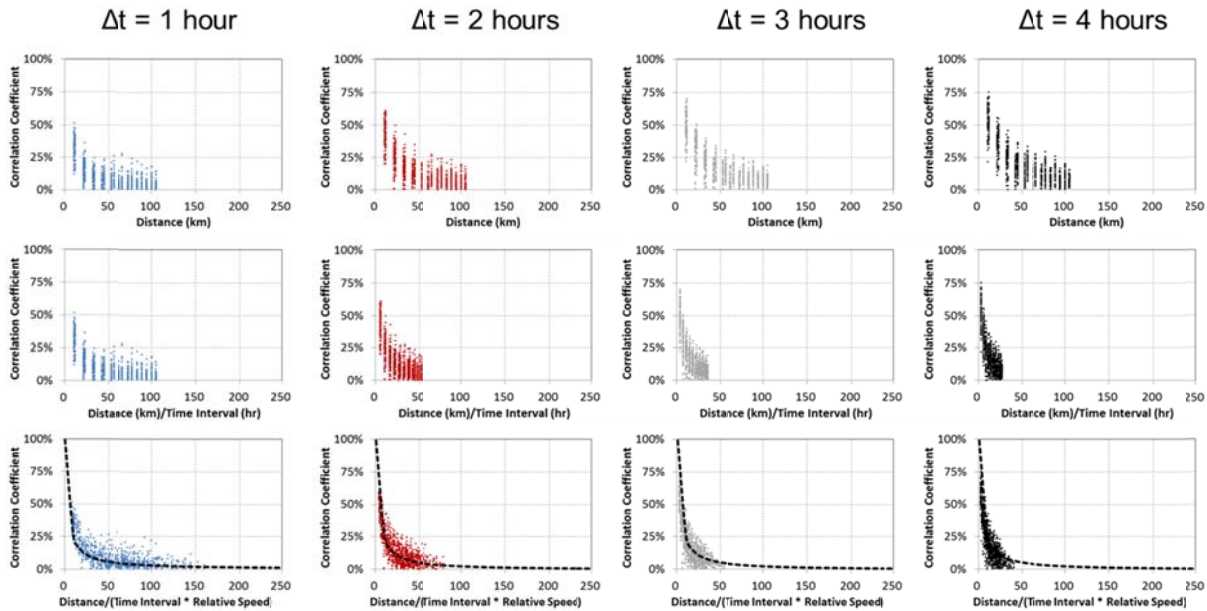
<sup>12</sup> Relative speed equals the implied speed derived for the specific location from SolarAnywhere data by the average implied speed across the entire geographic region. Relative speed is only used for presentation purposes for the benefit of the reader so that the scale of the x-axis remains constant.

Figure 4. Correlation coefficients presented by time interval for Great Plains.



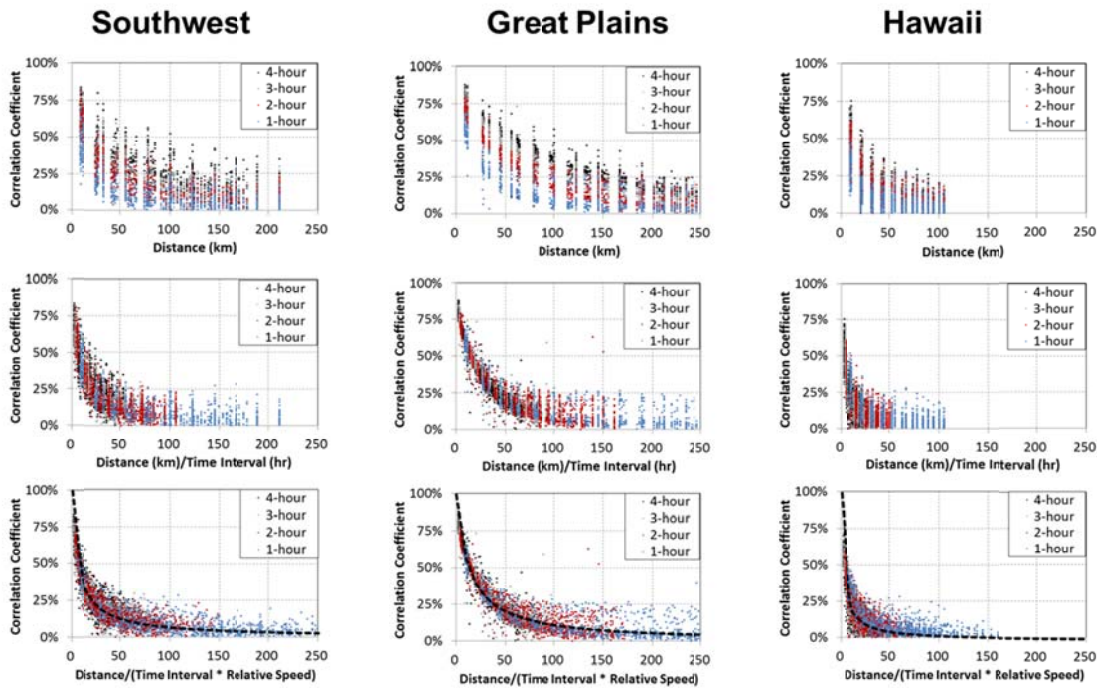
Note: Distance / (Time Interval \* Relative Speed) is related to Dispersion Factor

Figure 5. Correlation coefficients presented by time interval for Hawaii.



Note: Distance / (Time Interval \* Relative Speed) is related to Dispersion Factor

Figure 6. Correlation coefficients for all locations and time intervals.



Note: Distance / (Time Interval \* Relative Speed) is related to Dispersion Factor

## Discussion

The analysis provides several key findings. First, consistent with previous studies, the correlation coefficients decrease with increasing distance (top row of Figure 6). Second, also consistent with previous studies, this decrease occurs more slowly with longer time intervals (top row of Figure 6). An alternative way of viewing this result is that correlation coefficients decrease at a similar rate when plotted versus distance divided by time interval (middle row of Figure 6). Third, the scatter in results is further decreased when a relative speed<sup>12</sup> is introduced for the first location in the pair of locations (bottom row of Figure 6). Finally, the generalized method, shown by the dashed black line in the bottom row of Figure 6, fits the empirical data quite well when calibrated using the location-specific derived input parameters.

## Results Project to Shorter Time Intervals

An encouraging result of the foregoing analysis is the ability of the proposed general method, validated directly with several empirical data sets, to predict correlation coefficients with such accuracy. Even more encouraging is that the method is shown to be valid regardless of the selected time interval. While input data to the method was taken from the SolarAnywhere data set with a one-hour time interval, the method is shown to produce accurate correlation coefficients for one-hour, two-hour, three-hour, and four-hour time intervals. This finding prompted the authors to evaluate the potential of using the method based on parameters derived from the SolarAnywhere data set to project results to time intervals shorter than one hour.

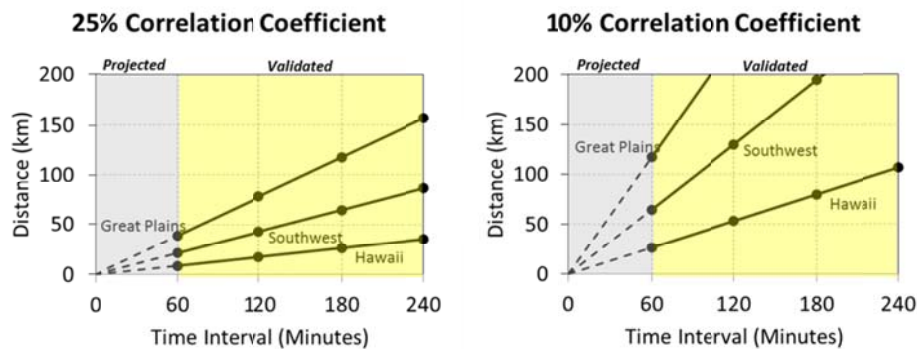
It would be a highly valuable finding if the method could be shown to produce accurate results for time intervals shorter than the available raw data. It would mean that the existing SolarAnywhere data set could be used to determine variability for fleets across the U.S., reducing the need for high-speed, high-resolution data that is currently unavailable.

While the desired objective is to demonstrate that the method accurately determines correlation coefficients (and therefore variability) as a function of PV spacing, a mathematically equivalent objective is to show that, for a given correlation coefficient, it is possible to accurately determine spacing between PV systems.

The circles in Figure 7 correspond to the method results taken from the dotted curve in the bottom row of Figure 6. For example, Figure 6 implies that PV systems need to be spaced 40 km apart in the Great Plains in order to achieve a 25 percent correlation coefficient using a 60 minute time interval. Triple the time interval to 180 minutes and plants need to be spaced triple the distance (120 km apart) to achieve the same 25 percent correlation coefficient.

The solid lines connecting the four time interval observations for each location in Figure 7 illustrate that the relationship is linearly related to the time interval. The figure begs the question as to whether the results can be projected in the region with shorter time intervals (i.e., the gray sections of the figures).

Figure 7. Results scale linearly with the time interval for a fixed correlation coefficient.



## Evaluation of Time-Independence Claim

The above linear relationship suggests that the method is independent of selected time interval, even down to the very short time intervals (several seconds to several minutes) that are of primary interest to the utilities. This section provides an initial validation of time-independence by comparing results calculated from the one-hour SolarAnywhere data set against results from independent studies that used 10-second, 20-second, and one-minute data sets.

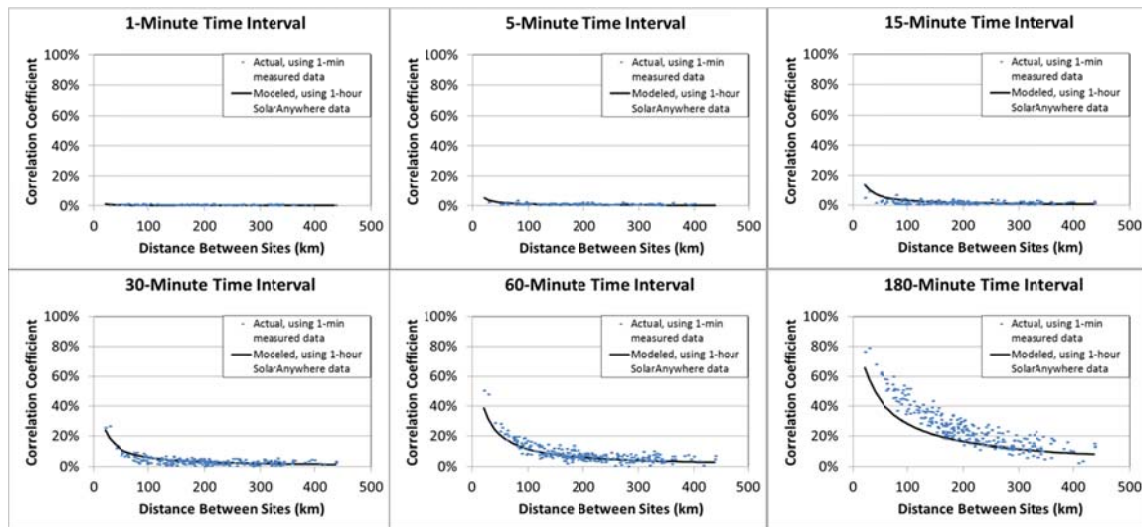
## Geographic Diversity Study

Mills and Wisner (2010) used measured one-minute insolation data for 23 time-synchronized sites in the Southern Great Plains network of the Atmospheric Radiation Measurement (ARM) program to



characterize the variability of PV with different degrees of geographic diversity. That report presented<sup>13</sup> the correlation of changes in global clear sky index between these geographically dispersed sites. Mills and Wiser provided an electronic version of their results and these were used to compare against the general method proposed here. While the one-hour SolarAnywhere data set was used as input to the general method, correlation coefficients were calculated that corresponded to much shorter time intervals in the Mills and Wiser study. The results, presented in Figure 8, are comparable to the Mills and Wiser study even down to one-minute time intervals.<sup>14</sup>

Figure 8. Comparison of results to geographic diversity study.



### Virtual Network Study

Perez et. al. (2010) obtained 20-second to one-minute insolation data for 24 measuring stations, including 17 stations in the ARM network and 7 stations in the SURFRAD network. They constructed one-dimensional virtual networks<sup>15</sup> using satellite-derived cloud speeds to translate time measurements into space measurements. They then calculated correlation coefficients between the change in clearness index for various time intervals and distances. Figure 9 presents some of the key results from that study. Figure 10 re-plots the data from the virtual network study along with corresponding projections from the current study (based on input parameters calculated one-hour SolarAnywhere data). Results compare well to virtual network study down to correlation coefficients of 40 percent for time intervals between 20 seconds to 15 minutes. Results from the virtual network study correlation coefficients below 40 percent may be lower as a result of the negative correlation arising from locations that are very close together.

<sup>13</sup> Figure 5 in Mills and Wiser (2010).

<sup>14</sup> The minor differences in 180-minute time intervals are due to methodological differences between the two studies.

<sup>15</sup> See Hoff and Perez (2010) for a discussion of virtual network construction.

Figure 9. Key results from virtual network study.

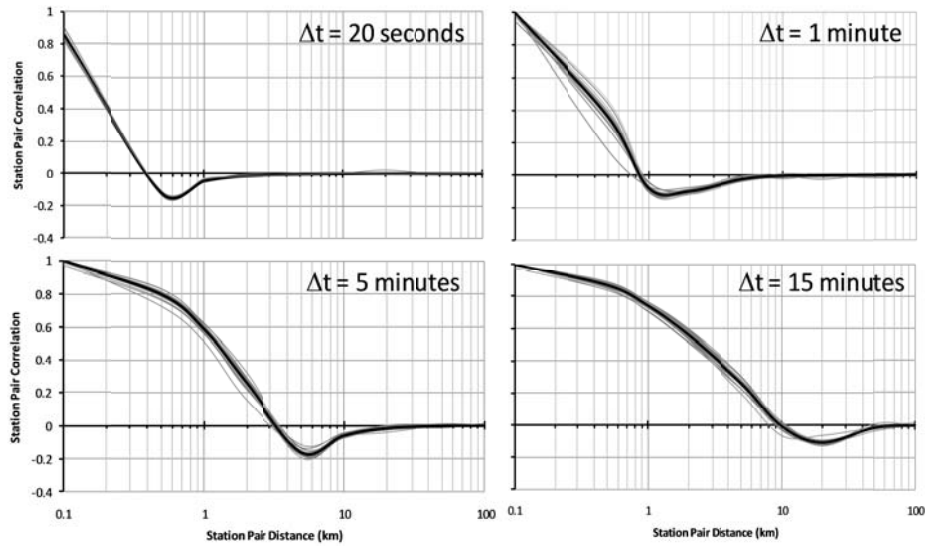
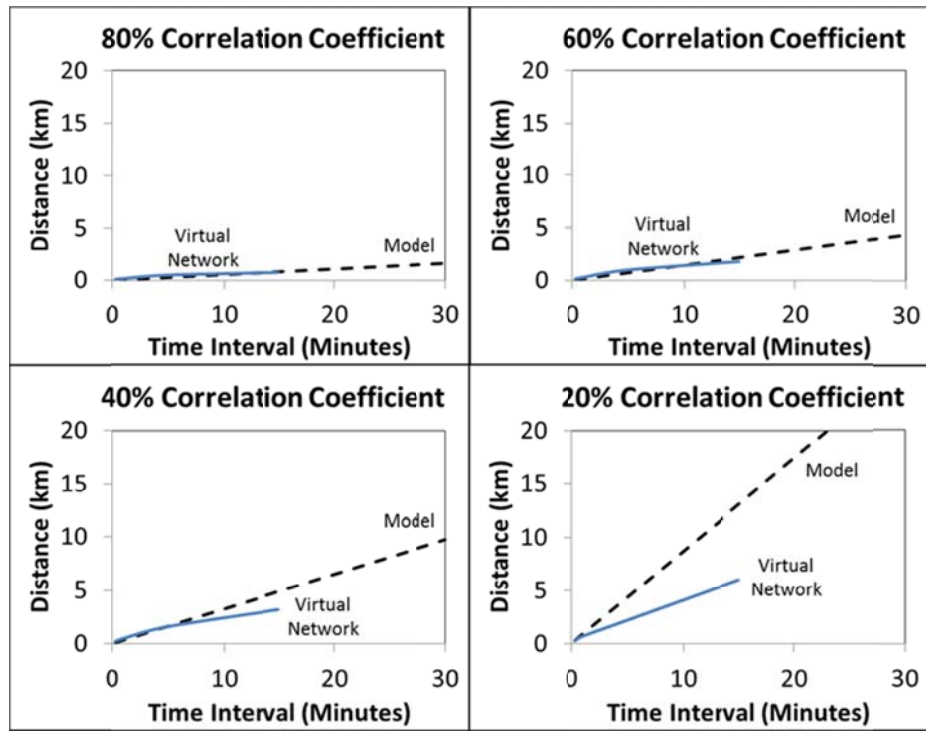


Figure 10. Comparison of results to virtual network study.



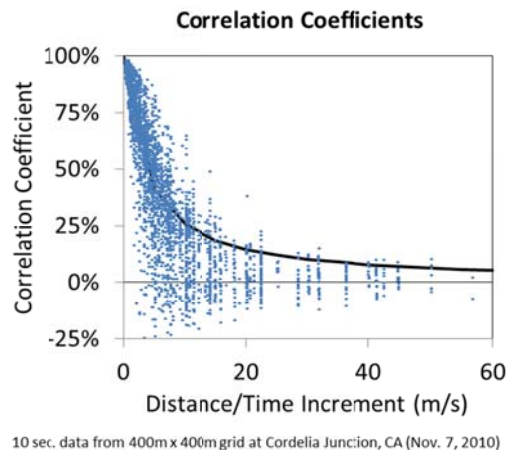
## High Density Weather Station Network

A third data set was provided by Hoff and Norris (2010). This data is from a network of 25 weather collection devices. This network is interesting from several perspectives. First, it is one of the few known high-density networks providing high speed data (see Kuszamaul 2010 for a network of 24 sensors in Lanai, HI). Second, it is designed to be deployed to multiple locations for short durations of time and thus is mobile.

This network was deployed at Cordelia Junction, CA in a 400-meter by 400-meter configuration (a square composed of 100 meters between stations). Figure 11 presents the correlation coefficients for November 7, 2010. The irradiance data associated with these coefficients is presented in Figure 1. Since there are 25 locations, there are 625 possible combinations, 300 of which are unique. Each of these combinations was evaluated using nine different time intervals (10, 20, 30, 40, 50, 60, 90, 120, and 300 seconds). Thus, there are 2,700 unique scenarios.

As can be seen by the black line in the figure, the results fits the empirical data fairly well. It is interesting to note that this data set exhibits some of the negative correlation effects identified by Hoff and Perez (2010) and Perez, et. al. (2010b) using the virtual network approach.

Figure 11. Correlation coefficients for high-density, 25 unit network at Cordelia Junction, CA on November 7, 2010 for time intervals from 10 seconds to 5 minutes.



## Conclusions

The objective of this paper was to lay the foundation for a new method that could be employed in future utility tools to enable the calculation of PV fleet variability for planning and operational purposes. The method used satellite-derived data and physical fleet parameters to determine correlation between PV sites, from which fleet variability can be derived.

The paper used hourly global horizontal insolation data from SolarAnywhere to validate the method by calculating correlation coefficients for 70,000 scenarios across three separate geographic regions in the United States (Southwest, Southern Great Plains, and Hawaii), while varying distance, time interval, insolation bin, and other parameters. These empirical correlation coefficients compared favorably with those derived by the method. The method was then shown to be independent of selected time interval, such that hourly satellite data could be used to calculate correlation coefficients for very short time intervals (several seconds to several minutes). These extrapolated results were validated using results from studies that are based on 20-second to one-minute insolation data.

The paper had several important findings. First, correlation coefficients decreased with increasing distance. Second, correlation coefficients decreased at a similar rate when plotted versus distance divided by time interval. Third, the accuracy of results was further improved when an implied speed term is introduced into the analysis. Together, these results provided the basis for validating the generalized method. The method, based on input parameters from hourly SolarAnywhere data, produced correlation coefficients for short time intervals (seconds to minutes) that compared quite well to results from independent studies that used 10-second, 20-second, and one-minute data sets.

The preliminary conclusion of this work is that the approach validated in this paper can be used to identify the conditions under which the change in output between locations are uncorrelated. As a result, it can be used to satisfy one of the initial motivations of this study: the desire to equip utility planners with a tool capable of placing an upper bound on the maximum output variability of a fleet of PV systems using a manageable amount of data and analysis.

The results, however, may have further implications. In particular, the results may be the basis for quantifying output variability even when correlation exists.

## Next Steps

This study demonstrated the ability to predict correlation coefficients using time intervals of 1 to 4 hours using multi-year data sets. Results also suggested that the method is valid for short time intervals when compared to high speed studies, again based on long time period data sets.

The next steps will be to further validate the results for short time intervals using measured higher speed data. Plans include the use of: 1 km x 1 km grid, ½-hour SolarAnywhere data in selected locations; 1 km x 1 km grid, one-minute extrapolated SolarAnywhere data in selected locations; and additional 10-second data from the mobile, high-density network described earlier (Hoff and Norris, 2010). A particularly important focus of this work will be to assess the method's ability to predict correlation between locations over short time periods as well as long time periods (several hours versus several years).

## Acknowledgements

Portions of this study were funded under a California Solar Initiative (CSI) Grant Agreement titled "Advanced Modeling and Verification for High Penetration PV." The California Public Utilities Commission is the Funding Approver, Itron is the Program Manager, and PG&E is the Funding

Distributor. Thanks to Ben Norris (Clean Power Research) who designed, implemented, and operated the mobile irradiance network and provided valuable comments on the paper. Thanks to Jeff Ressler (Clean Power Research) for his comments. Opinions expressed herein are those of the authors only.

## References

Hoff, T. E., Perez, R. 2010. Quantifying PV power Output Variability. *Solar Energy* 84 (2010) 1782–1793.

Hoff, T.E., Norris, B. 2010. Mobile High-Density Irradiance Sensor Network: Cordelia Junction Results.

Kuszamul, S., Ellis, A., Stein, J., Johnson, L. 2010. Lanai High-Density Irradiance Sensor Network for Characterizing Solar Resource Variability of MW-Scale PV System. 35<sup>th</sup> Photovoltaic Specialists Conference, Honolulu, HI. June 20-25, 2010.

Mills, A., Wiser, R. 2010. Implications of Wide-Area Geographic Diversity for Short-Term Variability of Solar Power. Lawrence Berkeley National Laboratory Technical Report LBNL-3884E.

Mills, A., Alstrom, M., Brower, M., Ellis, A., George, R., Hoff, T., Kroposki, B., Lenox, C., Miller, N., Stein, J., Wan, Y., 2009. Understanding variability and uncertainty of photovoltaics for integration with the electric power system. Lawrence Berkeley National Laboratory Technical Report LBNL-2855E.

Perez, R., Kivalov, S., Schlemmer, J., Hemker Jr., C. , Hoff, T. E. 2010a. Parameterization of site-specific short-term irradiance variability. Submitted to *Solar Energy*.

Perez, R., Kivalov, S., Schlemmer, J., Hemker Jr., C. , Hoff, T. E. 2010b. Short-term irradiance variability correlation as a function of distance. Submitted to *Solar Energy*.

Solar Anywhere\_, 2009. Web-Based Service that Provides Hourly, Satellite-Derived Solar Irradiance Data Forecasted 7 days Ahead and Archival Data back to January 1, 1998. [www.SolarAnywhere.com](http://www.SolarAnywhere.com).

Stokes, G.M., Schwartz, S.E., 1994. The atmospheric radiation measurement (ARM) program: programmatic background and design of the cloud and radiation test bed. *Bulletin of American Meteorological Society* 75, 1201–1221.

Wikipedia. 2010. [http://en.wikipedia.org/wiki/Correlation\\_and\\_dependence](http://en.wikipedia.org/wiki/Correlation_and_dependence).

Woyte, A., Belmans, R., Nijs, J. 2007. Fluctuations in instantaneous clearness index: Analysis and statistics. *Solar Energy* 81 (2), 195-206.

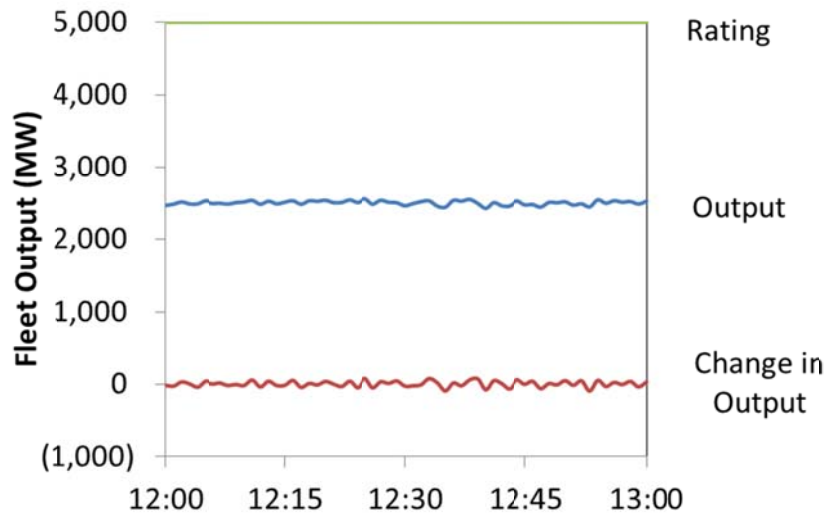
## Appendix A: Verification of Worst Case Scenario Results Using Excel

Table 7 and Figure 12 illustrate how to construct the worst case scenario using Excel. Construct a spreadsheet as shown in Table 7 by randomly generating either 0 or 1 for each minute for all 5,000 locations between 12:00 and 13:00. Sum the fleet output. Calculate the change in fleet output. Calculate output variability by calculating the standard deviation of the change in power.

Table 7. Worst case example for 5,000 independent 1 MW systems.

Time	Power (MW)						Change (MW/min)
	Plant #1	Plant #2	Plant #3	...	#5000	Fleet	
12:00	1	0	0	...	1	2,519	-33
12:01	0	0	1	...	0	2,552	-6
12:02	0	1	0	...	1	2,558	13
12:03	1	0	0	...	1	2,545	5
12:04	0	1	1	...	0	2,540	-12
...	...	...	...	...	...	...	...
13:00	0	1	1	...	0	2,525	

Figure 12. Simulated fleet output with maximum random variability.



## Appendix B

Table 8 and Figure 13 present three examples of how to calculate the change in the clearness index, which can then be used to calculate correlation coefficients.

Table 8. Data to calculate correlation coefficients.

Correlation coefficient equals 1.0								
Time	GHI (kW/m <sup>2</sup> )		Clear-Sky I (kW/m <sup>2</sup> )		Clearness Index		Change in Clearness Index	
	#1	#2	#1	#2	#1	#2	#1	#2
12:00	1.0	1.0	1.0	1.0	1.0	1.0	-1.0	-1.0
12:01	0.0	0.0	1.0	1.0	0.0	0.0	0.0	0.0
12:02	0.0	0.0	1.0	1.0	0.0	0.0	+1.0	+1.0
12:03	1.0	1.0	1.0	1.0	1.0	1.0	0.0	0.0
12:04	1.0	1.0	1.0	1.0	1.0	1.0		

Correlation coefficient equals 0.5								
Time	GHI (kW/m <sup>2</sup> )		Clear-Sky I (kW/m <sup>2</sup> )		Clearness Index		Change in Clearness Index	
	#1	#2	#1	#2	#1	#2	#1	#2
12:00	1.0	1.0	1.0	1.0	1.0	1.0	-1.0	0.0
12:01	0.0	1.0	1.0	1.0	0.0	1.0	0.0	-1.0
12:02	0.0	0.0	1.0	1.0	0.0	0.0	+1.0	+1.0
12:03	1.0	1.0	1.0	1.0	1.0	1.0	0.0	0.0
12:04	1.0	1.0	1.0	1.0	1.0	1.0		

Correlation coefficient equals 0								
Time	GHI (kW/m <sup>2</sup> )		Clear-Sky I (kW/m <sup>2</sup> )		Clearness Index		Change in Clearness Index	
	#1	#2	#1	#2	#1	#2	#1	#2
12:00	1.0	1.0	1.0	1.0	1.0	1.0	-1.0	0.0
12:01	0.0	1.0	1.0	1.0	0.0	1.0	0.0	-1.0
12:02	0.0	0.0	1.0	1.0	0.0	0.0	+1.0	0.0
12:03	1.0	0.0	1.0	1.0	1.0	0.0	0.0	+1.0
12:04	1.0	1.0	1.0	1.0	1.0	1.0		

Figure 13. Change in clearness index for Location 2 vs. Location 1.

